

Supporting Information

A Heavily Doped D-D' Type Polymer with Metal-like Carrier Transport by Hybrid Doping

Ayushi Tripathi,^a Yoonjoo Lee,^a Changhwa Jung,^b Soohyun Kim,^b Soonyong Lee,^a Woojin Choi,^b
Chaeyeon Park,^a Young Wan Kwon,^c Hyunjung Lee,^{*b} Han Young Woo^{*a}

^aDepartment of Chemistry, College of Science, Korea University, Seoul 02841, Republic of Korea

^bSchool of Materials Science and Engineering, Kookmin University, Seoul, 02707, Republic of
Korea

^cKU-KIST Graduate School of Converging Science and Technology, Korea University, Seoul
02841, Republic of Korea

*Corresponding authors.

E-mail address: hyunjung@kookmin.ac.kr (Hyunjung Lee), hywoo@korea.ac.kr (Han Young Woo)

1. Experimental

1.1 General

¹H and ¹³C NMR spectra were measured using a Bruker Advance III HD system operating at 500 and 125 MHz, respectively. Mass spectra were obtained using a MALDI-TOF/TOF™ 5800 system (AB SCIEX) at the Korea Basic Science Institute (KBSI). Molecular weight and dispersity of polymer were characterized by size exclusion chromatography (Agilent GPC 1200 series) with *o*-dichlorobenzene as the eluent at 80 °C relative to a polystyrene standard. Thermogravimetric analysis (TGA) and differential scanning calorimetry (DSC) measurements were conducted using a Scinco TGA N-1000 and PerkinElmer DSC 4000, respectively. UV–vis–NIR absorption spectra were measured by Cary 6000i UV–vis–NIR bundle (G9826A). Cyclic voltammetry (CV) was performed with a three-electrode cell (Versa STAT3, Princeton Applied Research) at a scan rate of 50 mV s⁻¹ in 0.1 M tetrabutylammonium tetrafluoroborate (Bu₄NBF₄) solution in CH₃CN: Ag/Ag⁺ as a reference electrode, a platinum electrode coated with a thin polymer film as the working electrode, and a platinum wire as a counter electrode. Electron paramagnetic resonance (EPR) spectra were obtained at the X-band frequency using a JES-FA200 (JEOL) electron spin resonance spectrometer. X-ray photoelectron spectroscopy (XPS) analysis was conducted with Al source on PHI's X-tool under UHV-17 Pa and at energy resolution less than 0.48–0.5 eV relative to Au. 2D grazing incidence wide-angle X-ray scattering (GIWAXS) was measured at beamline 9A (U-SAXS) at the Pohang Accelerator Laboratory (PAL) in Korea.

1.2. Synthesis

4,9-Bis(bis(hexylthio)methylene)-4,9-dihydro-s-indaceno[1,2-b:5,6-b']dithiophene (2).

Under nitrogen, 4,9-dihydro-s-indaceno[1,2-b:5,6-b']dithiophene (1 g, 3.75 mmol) and

potassium *tert*-butoxide (1.8 g, 16.14 mmol) were added to a 20 mL anhydrous dimethyl sulfoxide (DMSO) in a 100 mL two-neck round-bottom flask. Carbon disulfide (628 mg, 8.24 mmol) was injected to the above flask via syringe and the reaction mixture was stirred for 10 min. 1-Bromohexane (3.72 g, 22.52 mmol) was added dropwise to the reaction mixture and stirred at room temperature for 4 h. The mixture was quenched by adding cold water, extracted with 100 mL hexane four times and the combined organic layer was washed with 200 mL brine three times. The reaction mixture was dried over anhydrous Na₂SO₄, concentrated under reduced pressure, and purified by silica gel column chromatography (dichloromethane/hexane = 1:10, v:v) to afford a dark red sticky liquid (Yield: 84%). ¹H NMR (500 MHz, CDCl₃): δ (ppm) 8.85 (s, 2H), 7.98 (d, J = 5.0 Hz, 2H), 7.14 (d, J = 5 Hz, 2H), 3.05 (dd, 8H), 1.74-1.65 (m, 8H), 1.49-1.40 (m, 8H), 1.34-1.24 (m, 16H), 0.89-0.8 (m, 12H). ¹³C NMR (125 MHz, CDCl₃): δ (ppm) 144.65, 143.65, 139.14, 139.01, 137.59, 134.61, 125.60, 124.37, 117.46, 35.78, 35.18, 31.40, 30.17, 28.65, 22.59, 14.06.

4,9-Bis(bis(hexylthio)methylene)-4,9-dihydro-s-indaceno[1,2-b:5,6-b']dithiophene-2,7-diyl-bis(trimethylstannane) (M1). Under nitrogen, 2,2,6,6-tetramethylpiperidine (0.93 g, 6.61 mmol) was dissolved in dry tetrahydrofuran (THF) in a 100 mL two-neck round-bottom flask and 2.5 M *n*-BuLi in hexane (2.65 mL, 6.61 mmol) was added to it. The reaction mixture was cooled down to -78 °C. Compound 2 (1 g, 1.32 mmol) was dissolved in THF (10 mL), which was injected dropwise to the above reaction mixture, followed by stirring at -78 °C. After 2 h, 1 M trimethylstannyl chloride solution in THF (6.62 mL, 6.61 mmol) was added and the reaction mixture was stirred at -78 °C for another 2 h. The mixture was quenched by cold water, extracted with 100 mL ether four times and the combined organic phases were washed with 200 mL brine three times. The reaction mixture was dried over anhydrous Na₂SO₄, concentrated under reduced

pressure and recrystallized from ethanol to give a red solid (Yield: 72%). ¹H NMR (500 MHz, CDCl₃): δ (ppm) 8.79 (s, 2H), 8.00 (s, 2H), 3.03 (m, 8H), 1.73-1.66 (m, 8H), 1.49–1.42 (m, 8H), 1.34-1.24 (m, 16H), 0.89-0.8 (m, 12H), 0.41 (s, 18H). ¹³C NMR (126 MHz, CDCl₃): δ (ppm) 150.74, 145.78, 139.37, 138.28, 137.65, 137.48, 134.40, 133.00, 117.77, 35.81, 35.11, 31.41, 30.11, 28.63, 22.59, 14.03. MS (MALDI-TOF) m/z: [M⁺] Calcd for C₄₈H₇₄S₆Sn₂, 1080.22; found, 1080.15.

4-(Bis(2-hexyldecylthio)methylene)-4H-cyclopenta[2,1-b:3,4-b']dithiophene (4). In a nitrogen atmosphere, cyclopenta[2,1-b:3,4-b']dithiophene (1 g, 5.61 mmol) was dissolved in dry DMSO and sodium *tert*-butoxide (1.1 g, 12.34 mmol) was added. After the reagents were completely dissolved, carbon disulfide (472 mg, 6.73 mmol) was injected to the above flask via syringe and the reaction mixture was stirred for 10 min. Hexyldecyl bromide (3.6 g, 12.34 mmol) was added dropwise to the reaction mixture and stirred at room temperature for 4 h. The mixture was quenched by adding cold water and extracted with 100 mL dichloromethane (DCM) four times. The combined organic layer was washed with 200 mL brine three times, dried over anhydrous Na₂SO₄, concentrated under reduced pressure, and purified by silica gel column chromatography (hexane) to afford dark red sticky liquid (Yield: 68%). ¹H NMR (500 MHz, CDCl₃): δ (ppm) 7.88 (d, J = 5.0 Hz, 2H), 7.03 (d, J = 5.0 Hz, 2H), 2.99 (d, J = 5.0 Hz, 4H), 1.64 (m, 2H), 1.45–1.19 (m, 48H), 0.87 (m, 12H). ¹³C NMR (125 MHz, CDCl₃): δ (ppm) 143.95, 141.17, 137.84, 134.80, 125.38, 122.99, 39.55, 38.59, 33.28, 31.90, 31.83, 29.96, 29.62, 29.58, 29.35, 26.63, 22.69, 14.11.

4-(Bis(2-hexyldecylthio)methylene)-2,6-dibromo-4H-cyclopenta[2,1-b:3,4-b']dithiophene (M2). In a 100 mL one-necked flask, compound 4 (1 g, 1.42 mmol) was dissolved in 10 mL *N,N*-dimethylformamide (DMF). The flask was covered with aluminum foil

to block the light and *N*-bromosuccinimide (0.53 g, 2.98 mmol) was added in portions to the above reaction mixture at 0 °C. The reaction mixture was stirred for 2 h at room temperature. The mixture was quenched by adding cold water and extracted with 100 mL DCM four times. The combined organic layer was washed with 200 mL brine three times, dried over anhydrous Na₂SO₄, concentrated under reduced pressure and purified by silica gel column chromatography (hexane) to afford dark red sticky liquid (Yield: 73 %). ¹H NMR (500 MHz, CDCl₃): δ (ppm) 7.88 (s, 2H), 2.98 (d, J = 5.0 Hz, 4H), 1.61 (m, 2H), 1.45–1.19 (m, 48H), 0.87 (m, 12H). ¹³C NMR (125 MHz, CDCl₃): δ (ppm) 144.95, 141.21, 137.22, 133.45, 128.04, 109.4539.55, 38.59, 33.28, 31.90, 31.83, 29.96, 29.62, 29.58, 29.35, 26.63, 22.69, 14.11. MS (MALDI-TOF) m/z: [M⁺] Calcd for C₄₂H₆₈S₄Br₂, 860.26; found, 860.23.

PIDTSCDTS. M1 (0.1 g, 0.092 mmol), M2 (0.080 g, 0.092 mmol), Pd₂(dba)₃ (2 mol%), P(*o*-tol)₃ (16 mol%) were added to a reaction flask and sealed tightly in a glove box. To the reaction mixture, 0.8 mL toluene was injected by syringe and stirred at 100 °C for 24 h. The polymerization solution was cooled down to room temperature and 2-tributylstannylthiophene (0.1 mL) was added and further reacted at 100 °C for 1 h for end-capping. The end-capping was repeated similarly with 2-bromothiophene (0.2 mL). The polymerization solution was precipitated into methanol, collected by filtration, and purified by Soxhlet extraction with methanol, acetone, and n-hexane. The chloroform portion containing the dissolved polymers was concentrated and re-precipitated into methanol, filtered and dried under vacuum (Yield: 94%). ¹H NMR (500 MHz, CDCl₃): δ (ppm) 8.75 (s, 2H), 8.75 (s, 2H), 8.11 (s, 2H), 8.00 (s, 2H), 3.06 (br, 12H), 1.74 (br, 8H), 1.53-1.16 (m, 74H), 0.96-0.77 (br, 24H).

1.3 Preparation of PIDTSCDTS films doped with FeCl₃ or AuCl₃

The polymer solution (8 mg mL^{-1}) in chloroform (Sigma-Aldrich, anhydrous, $\geq 99.9\%$) was prepared. The glass substrates ($2 \times 1 \text{ cm}$) were cleaned by acetone, isopropyl alcohol, and deionized water in an ultrasonic bath for 15 min each, dried using nitrogen (N_2) gas and then treated with UV-ozone for 10 min. Polymer films were prepared by spin-coating with a thickness of 80~100 nm. Lewis acid dopants, FeCl_3 and AuCl_3 were purchased from Alfa Aesar and Sigma-Aldrich and used without further purification. In a SqD method, dopant solutions were prepared by dissolving FeCl_3 or AuCl_3 in acetonitrile (Alfa Aesar, anhydrous, 99.8+%) ($[\text{AuCl}_3] = 0.01\text{--}30 \text{ mM}$ and $[\text{FeCl}_3] = 5\text{--}100 \text{ mM}$). The polymer solution was spin-coated and subsequently the dopant solution in acetonitrile was dropped onto the polymer films and allowed to stand for 10 s before spin-casting. In a MxD method, each dopant was dissolved in THF (Sigma Aldrich, anhydrous, $\geq 99.9\%$) with changing $[\text{AuCl}_3] = 5\text{--}50 \text{ mM}$ and $[\text{FeCl}_3] = 1\text{--}50 \text{ mM}$. Then, the blend was prepared by mixing polymer and dopant solutions at optimized ratio of 2:1 (v/v) to prevent aggregation and spin cast onto a glass substrate. For a HyD method, the polymer:dopant blend film was firstly prepared at a MxD stage ($[\text{AuCl}_3] = 0.05 \text{ mM}$ and $[\text{FeCl}_3] = 0.5 \text{ mM}$). Then, a dopant solution in acetonitrile was over-coated ($[\text{AuCl}_3] = 0.1\text{--}30 \text{ mM}$ and $[\text{FeCl}_3] = 1\text{--}80 \text{ mM}$).

1.4 Electrical conductivity and Seebeck coefficient measurement

Electrical conductivity was obtained by the four-point probe method using the current source meter (Keithley 2400). The Seebeck coefficient, S was obtained by measuring the potential difference (ΔV) by nanovolt meter (Agilent 34420A) under a temperature gradient ($\Delta T = \pm 1\text{--}3 \text{ K}$) in ambient condition. The slope ($\Delta V/\Delta T$) yielded the Seebeck coefficient. The detailed procedure can be found in a previous report.¹ The temperature dependence of electrical conductivity was measured by varying the temperature from 150 K to 350 K. The reduced activation energy $W(T)$

was calculated from Zabrodskii plot using equation (S1), where σ and T are the electrical conductivity and temperature, respectively.^{2,3}

$$W(T) = \frac{d \ln \sigma(T)}{d \ln T} \quad (\text{S1})$$

1.5 Metal-insulator-semiconductor (MIS) measurement

To investigate the charge carrier generation of chemically-doped PIDTSCDTS films depending on the doping methods, MIS devices were prepared. The doped polymer films to show the maximum σ were prepared on a Si/SiO₂ (200 nm thick) substrate by spin-coating as described above. Subsequently, the gate electrode (150 nm thick Au) was deposited on a doped polymer film by e-beam & thermal evaporation (08-065, Infovion) using a shadow mask (2.5×1 mm²). The capacitance–voltage characteristics of the MIS devices were obtained at a frequency of 100 Hz using an LCR meter (Agilent 4284A).

1.6 Charge transport analysis of doped PIDTSCDTS films by Kang-Snyder model

Kang-Snyder defined the transport function $\sigma_E(E,T)$ using generalized Boltzmann transport Equations S2 and S3,

$$\sigma = \int \sigma_E \left(-\frac{\partial f}{\partial E} \right) dE \quad (\text{S2})$$

$$\sigma_E(E,T) = \begin{cases} \sigma_{E0}(T) \times \left(\frac{E - E_t}{k_B T} \right)^s & (E > E_t) \\ 0 & (E < E_t) \end{cases} \quad (\text{S3})$$

where $\sigma_{E0}(T)$ is a transport coefficient, which is a temperature-dependent but energy-independent parameter, E_t is a transport edge, and s is a transport parameter. The S is also predicted by the transport function $\sigma_E(E,T)$ as Equation S4.

$$S = \frac{1}{\sigma} \left(\frac{k_B}{q} \right) \int \left(\frac{E - E_F}{k_B T} \right) \sigma_E \left(- \frac{\partial f}{\partial E} \right) dE \quad (\text{S4})$$

The σ and S can be simplified as Equations S5 and S6,

$$\sigma = \sigma_{E0}(T) \times sF_{s-1}(\eta) \quad (\text{S5})$$

$$S = \frac{k_B}{q} \left[\frac{(s+1)F_s(\eta)}{sF_{s-1}(\eta)} - \eta \right] \quad (\text{S6})$$

where $F_i(\eta)$ is the non-normalized complete Fermi-Dirac integral, and

$$\eta = \frac{E_F - E_t}{k_B T} \quad \text{is reduced chemical potential.}$$

2. Supplementary Figures and Tables

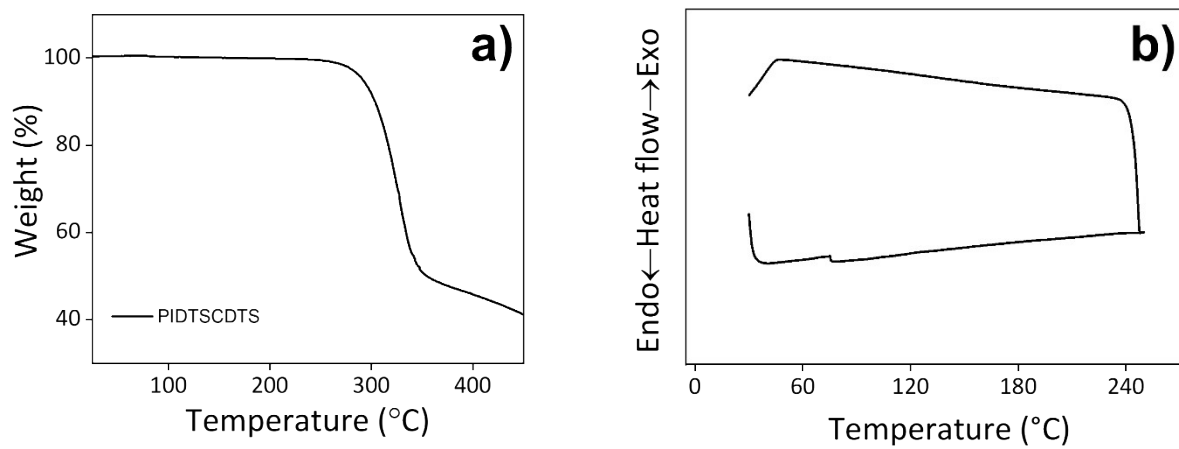


Fig. S1. (a) TGA, and (b) DSC thermograms of PIDTSCDTS.

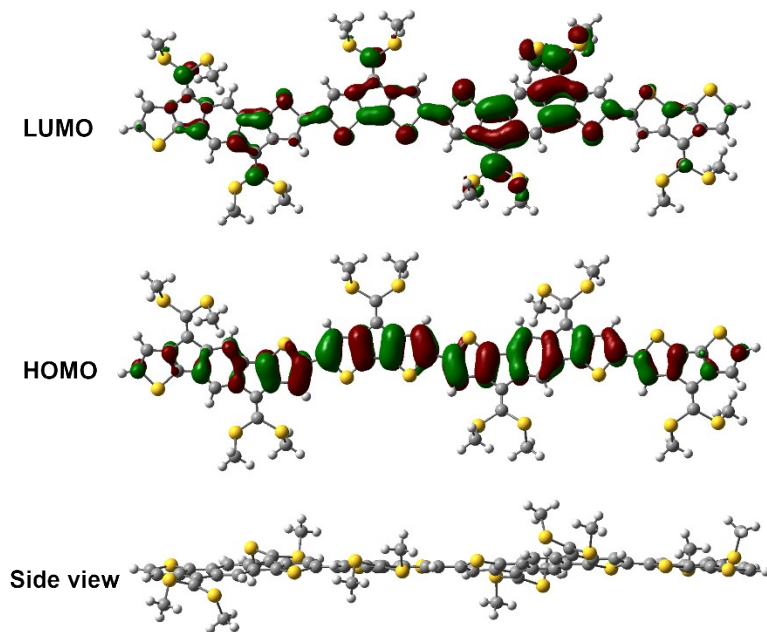


Fig. S2. DFT calculated frontier molecular orbital structures and energy-minimized conformation of PIDTSCDTS.

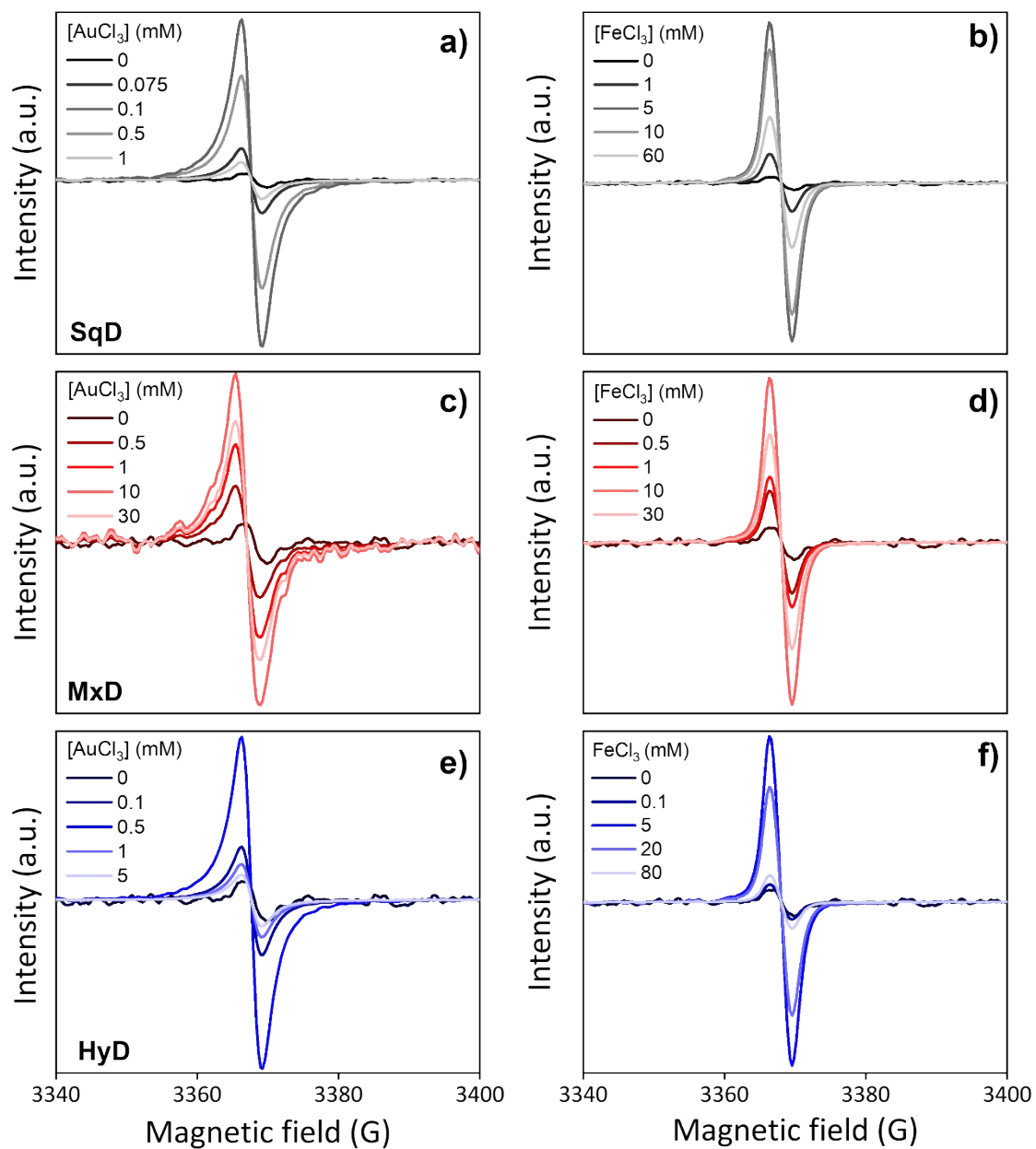


Fig. S3. EPR spectra of PIDTSCDTS doped with (a,b) SqD, (c,d) MxD, and (e,f) HyD as a function of AuCl_3 and FeCl_3 .

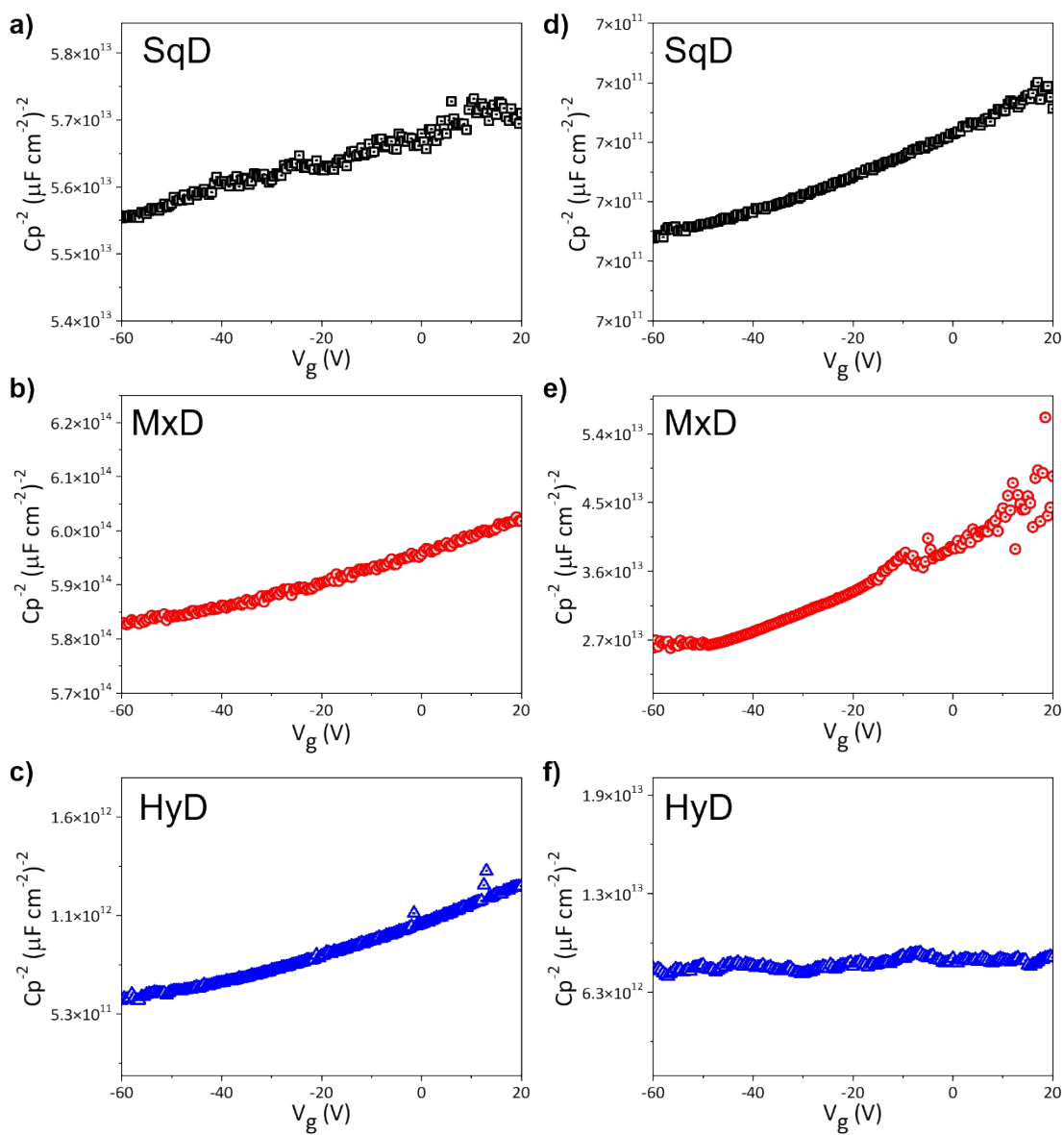


Fig. S4. Capacitance–voltage characteristics of (a–c) AuCl₃- and (d–e) FeCl₃-doped PIDTSCDTS films using three doping methods at σ_{max} .

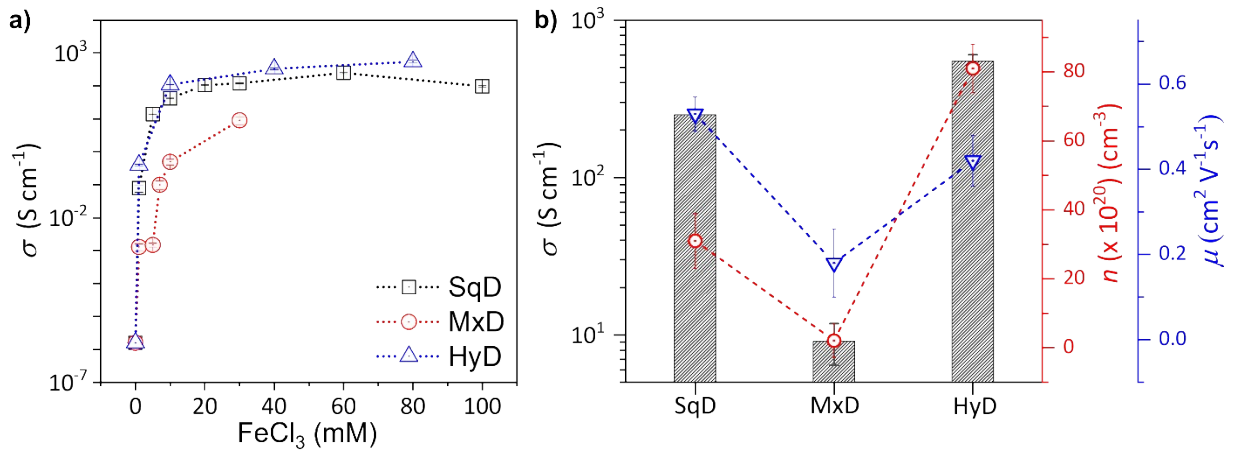


Fig. S5. (a) σ values as a function of the dopant concentration for FeCl_3 -doped PIDTSCDTS films by three doping methods. (b) Comparison of n and μ values at σ_{max} for FeCl_3 -doped PIDTSCDTS films.

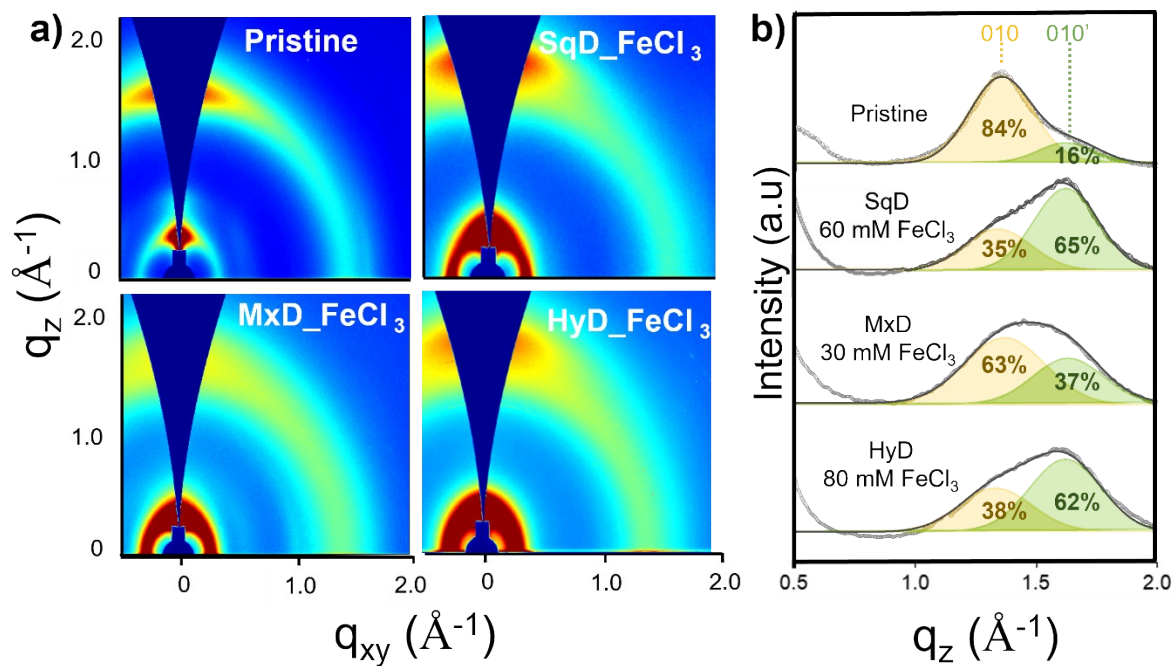


Fig. S6. 2-D GIWAXS images and out-of-plane line-cut profiles of pristine and FeCl₃-doped PIDTSCDTS films depending on three different doping methods.

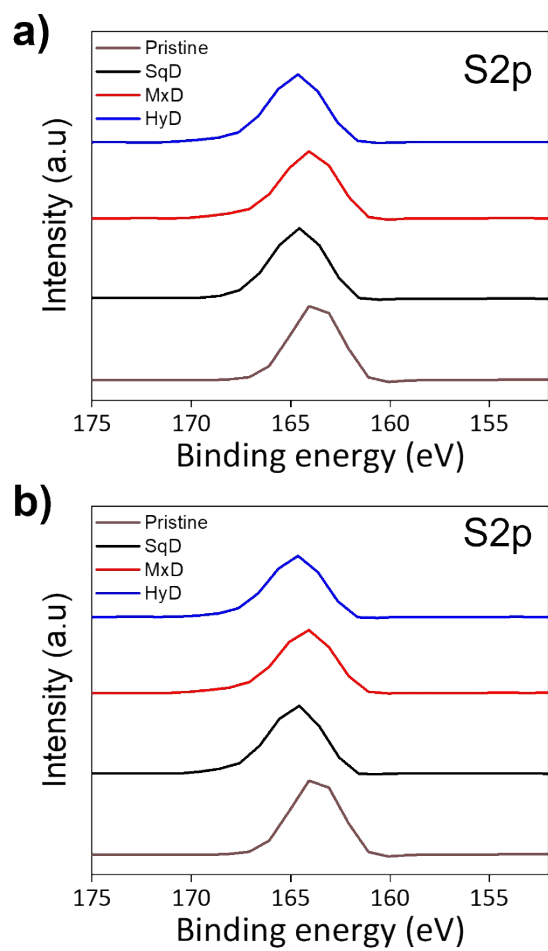


Fig. S7. XPS spectra of S 2p peaks of (a) AuCl₃-doped and (b) FeCl₃-doped PIDTSCDTS films by SqD, MxD and HyD.

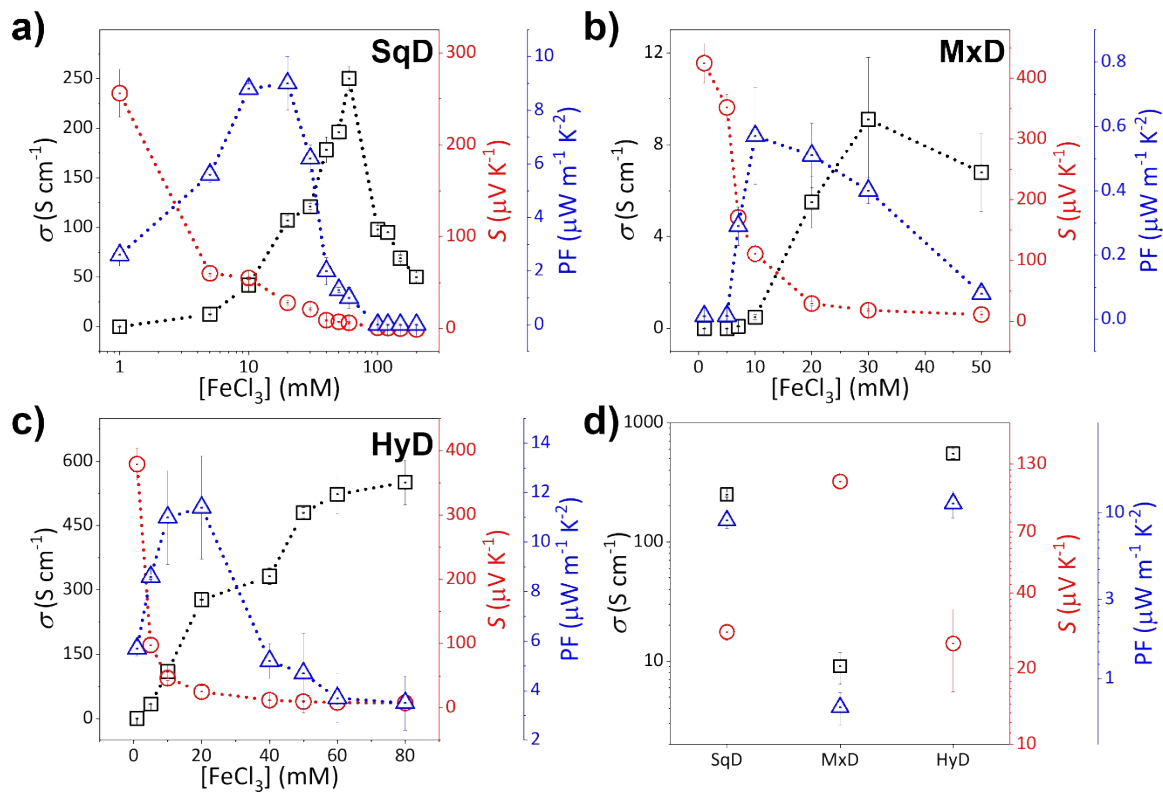


Fig. S8. Thermoelectric characteristics of FeCl₃-doped PIDTSCDTS films by (a) SqD, (b) MxD, and (c) HyD. (d) Maximum σ , PF and S (at maximum PF) values depending on doping methods. The dopant concentrations mentioned for HyD are those of overcoated dopant solutions after MxD at [FeCl₃] = 0.5 mM.

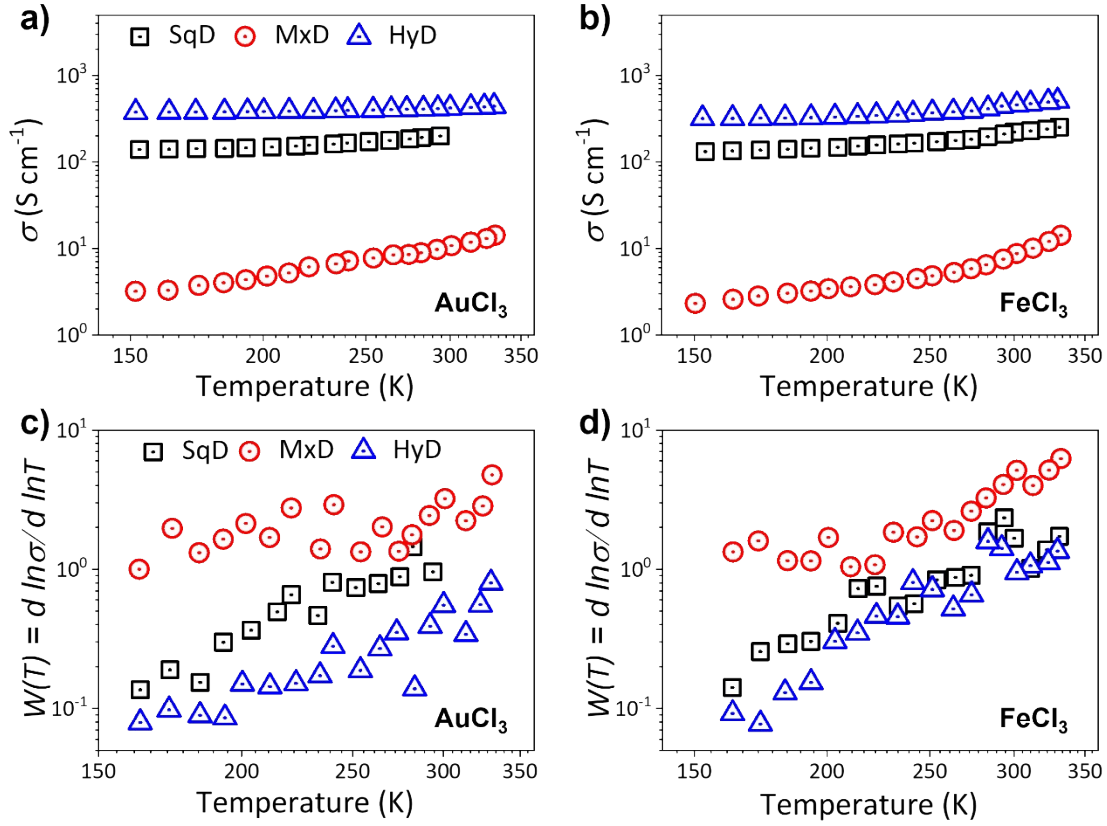


Fig. S9. Temperature-dependent electrical conductivity for (a) AuCl₃- and (b) FeCl₃-doped films at a dopant concentration that yielded the maximum electrical conductivity by SqD, MxD, and HyD. The reduced activation energy $W(T)$ versus temperature for (c) AuCl₃- and (d) FeCl₃-doped films depending on the doping methods.

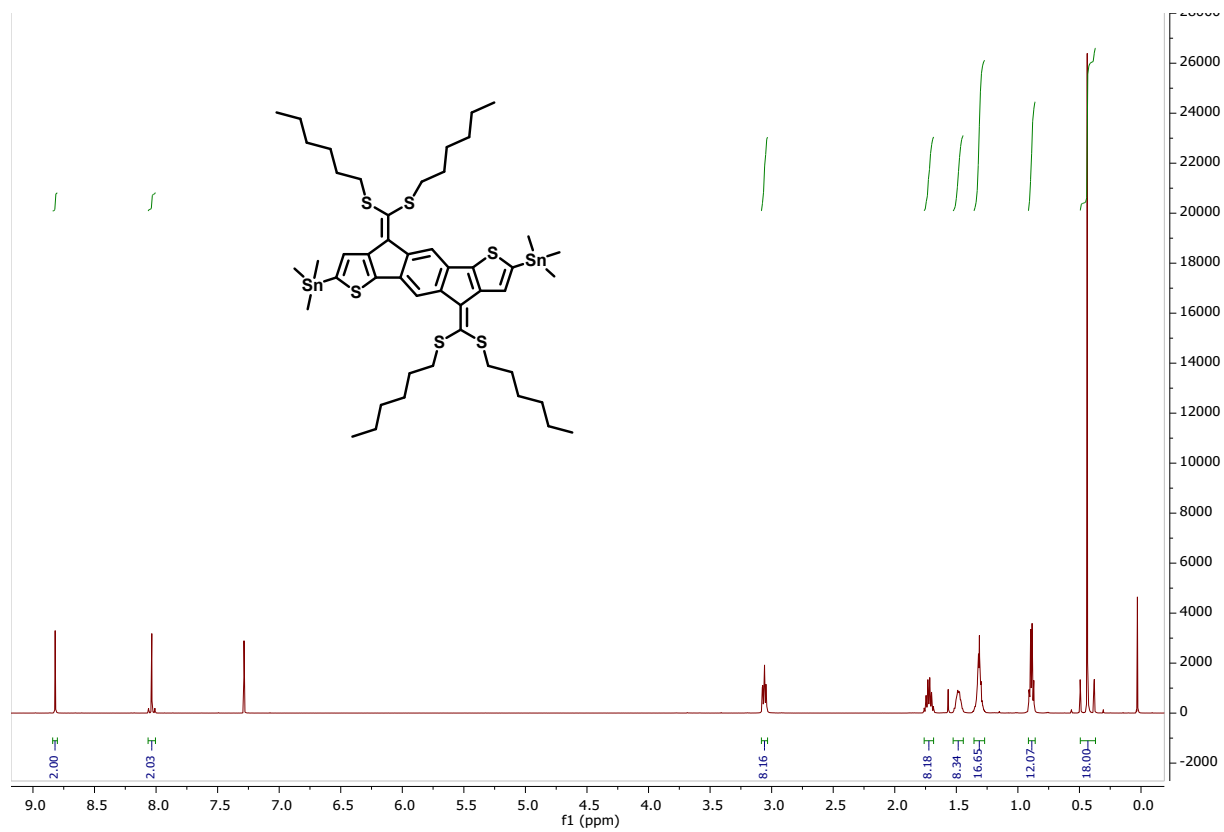


Fig. S10. ¹H NMR spectrum of compound M1 in CDCl₃.

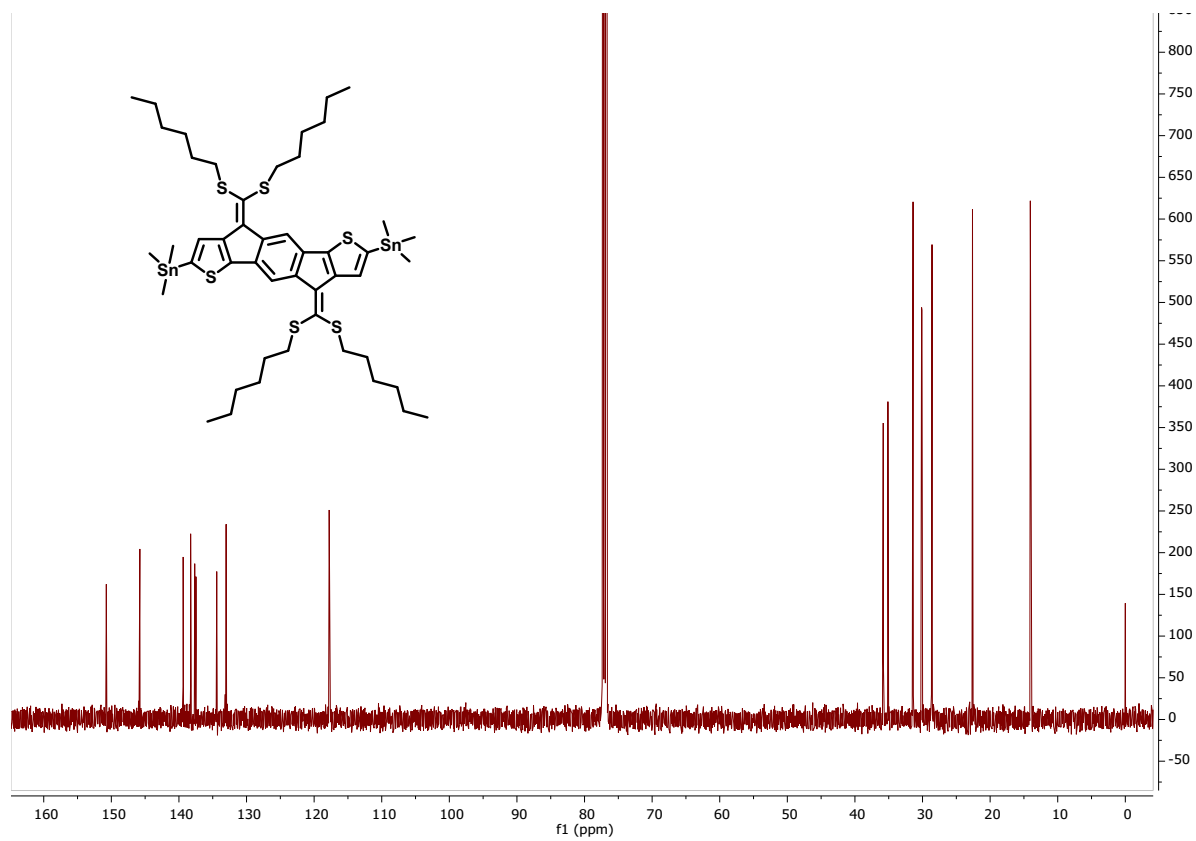


Fig. S11. ^{13}C NMR spectrum of compound M1 in CDCl_3 .

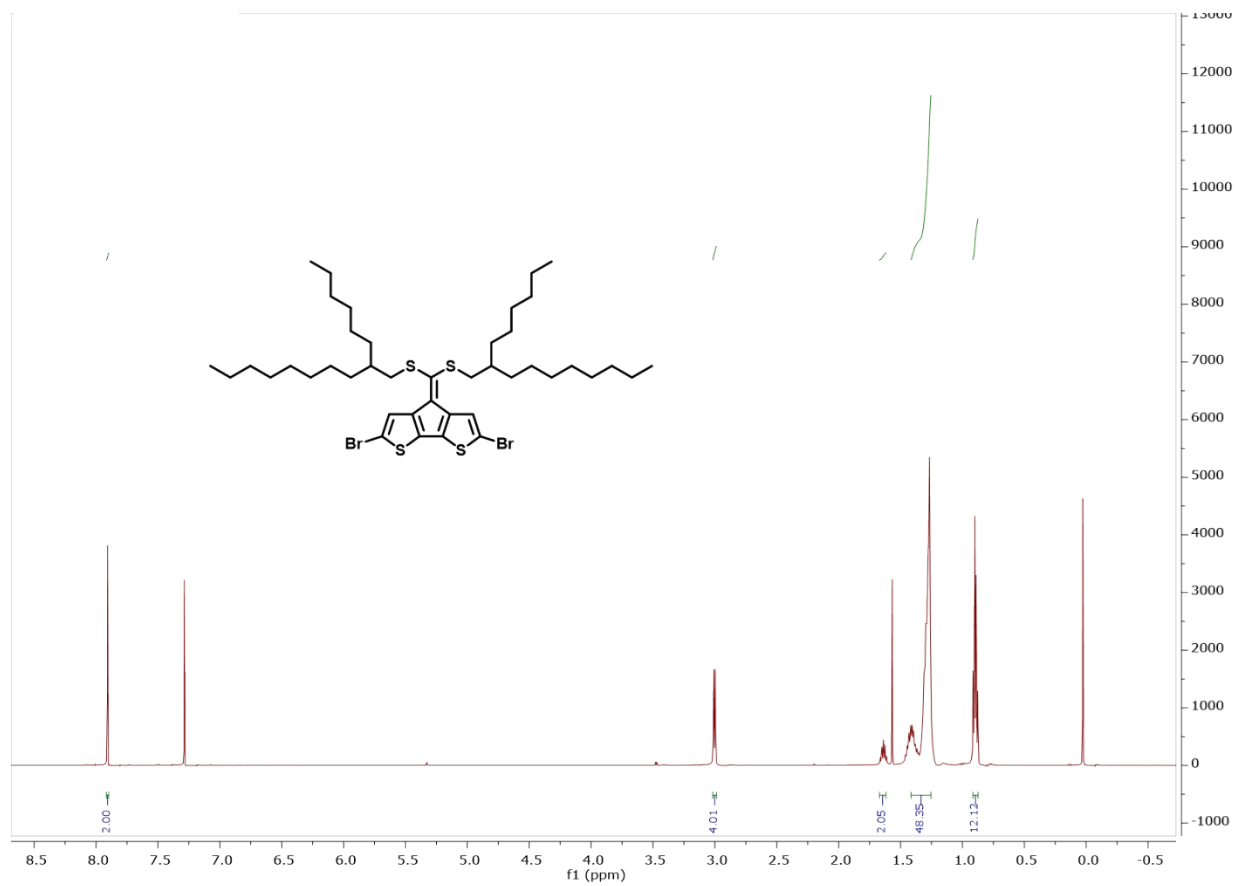


Fig. S12. ^1H NMR spectrum of M2 in CDCl_3 .

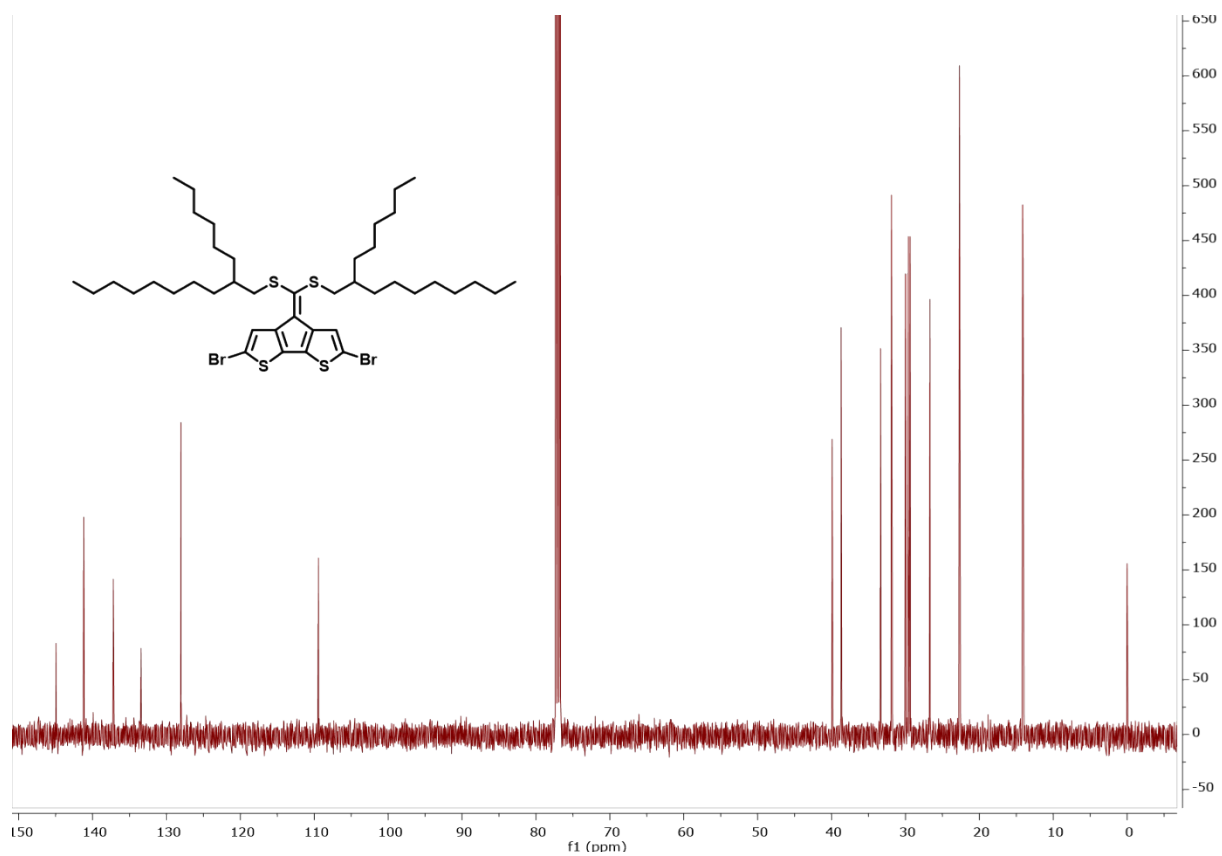


Fig. S13. ^{13}C NMR spectrum of M2 in CDCl_3 .

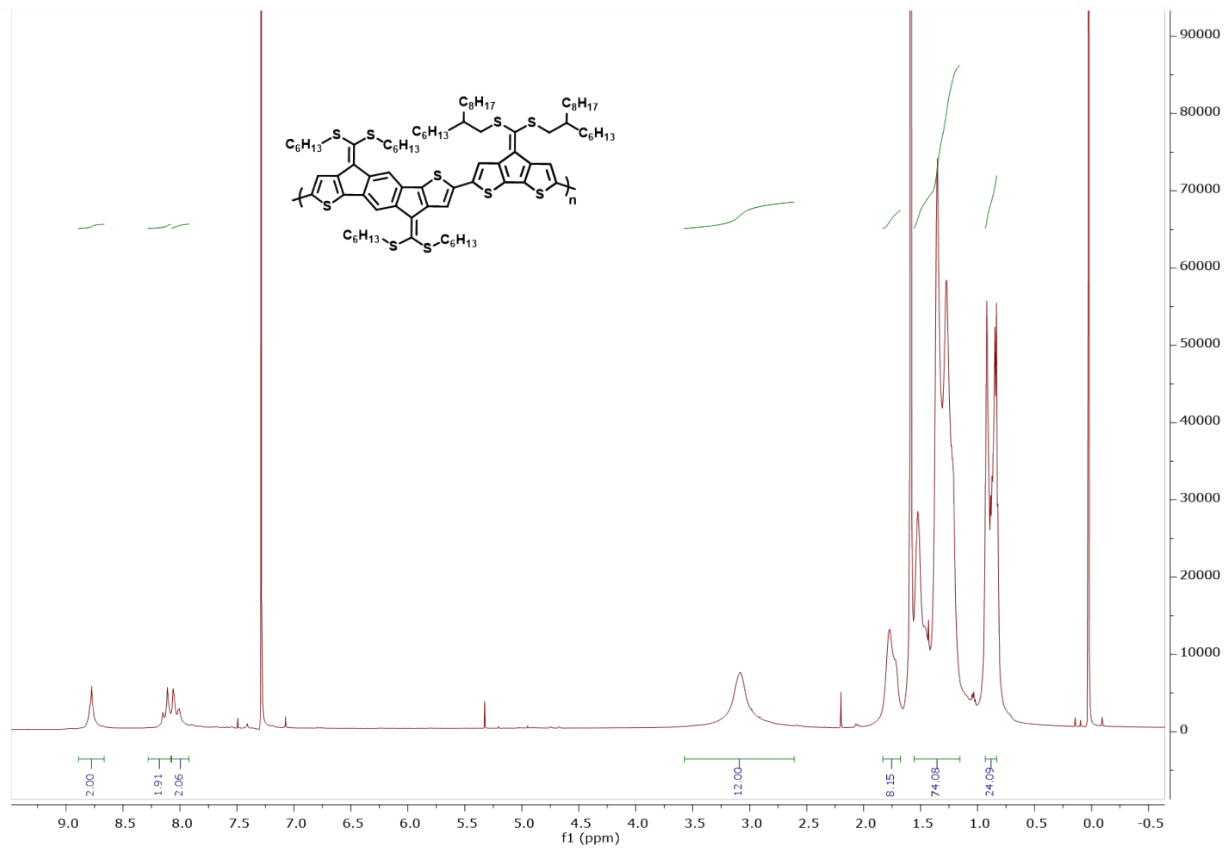


Fig. S14. ^1H NMR spectrum of PIDTSCDTS in CDCl_3 .

Table S1. Polaron density measurements of AuCl₃- and FeCl₃-doped PIDTSCDTS films as a function of dopant concentration by SqD, MxD, and HyD.

SqD			
[AuCl ₃] (mM)	Polaron density × 10 ¹⁸ (cm ⁻³)	[FeCl ₃] (mM)	Polaron density × 10 ¹⁸ (cm ⁻³)
0.075	4.20	1	2.56
0.1	5.53	5	5.71
0.5	4.80	10	4.86
1	3.38	60	3.94
MxD			
[AuCl ₃] (mM)	Polaron density × 10 ¹⁸ (cm ⁻³)	[FeCl ₃] (mM)	Polaron density × 10 ¹⁸ (cm ⁻³)
0.5	1.16	0.5	1.38
1	2.57	1	1.94
10	4.60	10	4.91
30	4.22	30	4.02
HyD			
[AuCl ₃] (mM)	Polaron density × 10 ¹⁸ (cm ⁻³)	[FeCl ₃] (mM)	Polaron density × 10 ¹⁸ (cm ⁻³)
0.1	5.92	0.1	1.44
0.5	6.11	5	7.28
1	0.95	20	6.49
5	0.68	80	1.13

Table S2. Summary of thermoelectric parameters of FeCl₃-doped polymer films.

Doping method	[FeCl ₃] (mM)	σ (S cm ⁻¹)	S (μ V K ⁻¹)	PF (μ W m ⁻¹ K ⁻²)
SqD	5	14 (± 0.5)	60 (± 2.6)	5.6 (± 0.3)
	10	42 (± 1)	55 (± 1.4)	8.8 (± 0.2)
	20	107 (± 5)	28 (± 2.1)	9.0 (± 1.0)
	30	121 (± 3)	21 (± 2)	6.2 (± 0.5)
	60	250 (± 12)	6.2 (± 1.2)	1.0 (± 0.4)
	100	98 (± 4.1)	0.9 (± 0.1)	8×10^{-3} ($\pm 2 \times 10^{-3}$)
MxD	7	0.10 (± 0.03)	171 (± 17)	0.29 (± 0.06)
	10	0.5 (± 0.1)	111 (± 7)	0.57 (± 0.15)
	30	9.1 (± 2.7)	18 (± 3)	0.40 (± 0.04)
	50	6.8 (± 1.7)	11 (± 4)	0.08 (± 0.02)
HyD	10	51.2 (± 0.1)	46.3 (± 3.9)	11.0 (± 1.9)
	20	152 (± 1)	25.2 (± 9.0)	11.4 (± 2.1)
	40	332 (± 19)	12.2 (± 1.0)	5.2 (± 0.7)
	60	523 (± 46)	8.3 (± 1.2)	3.7 (± 1.0)
	80	551 (± 52)	7.7 (± 1.1)	3.5 (± 1.1)

Table S3. GIWAXS packing parameters of AuCl₃- and FeCl₃-doped PIDTSCDTS films by SqD, MxD, and HyD.

Dopant (mM)	q_z (Å ⁻¹)	d -spacing (Å)	FWHM (Å ⁻¹)	CCL (Å)	Peak integration ratio (%)
0	1.40	4.5	0.30	18.7	83.7
	1.71	3.7	0.25	22.3	16.3
SqD 1mM AuCl ₃	1.40	4.5	0.34	16.4	36.6
	1.71	3.7	0.34	16.4	63.4
SqD 60 mM FeCl ₃	1.40	4.5	0.32	17.3	34.7
	1.71	3.7	0.31	18.2	65.3
MxD 30 mM AuCl ₃	1.40	4.5	0.33	17.1	55.1
	1.71	3.7	0.32	17.5	44.9
MxD 30 mM FeCl ₃	1.40	4.5	0.39	14.3	63.0
	1.71	3.7	0.34	16.7	37.0
HyD 5 mM AuCl ₃	1.40	4.5	0.34	16.6	51.0
	1.71	3.7	0.31	18.0	49.0
HyD 80 mM FeCl ₃	1.40	4.5	0.35	16.1	37.8
	1.71	3.7	0.34	16.4	62.2

References:

- 1 H. Bark, J. Lee, H. Lim, H. Y. Koo, W. Lee and H. Lee, *ACS Appl. Mater. Interfaces*, 2016, **8**, 31617–31624.
- 2 Y. Lee, J. Park, J. Son, H. Young Woo, J. Kwak, Y. Lee, J. Son, H. Y. Woo, J. Park and J. Kwak, *Adv. Funct. Mater.*, 2021, **31**, 2006900.
- 3 X. Wang, X. Zhang, L. Sun, D. Lee, S. Lee, M. Wang, J. Zhao, Y. Shao-Horn, M. Dincă, T. Palacios and K. K. Gleason, *Sci. Adv.*, , DOI:10.1126/sciadv.aat5780.